Respiratory Physiology & Neurobiology 265 (2019) 9–18

Contents lists available at ScienceDirect

Respiratory Physiology & Neurobiology

journal homepage: www.elsevier.com/locate/resphysiol

Microglial modulators reduce respiratory rhythm long-term facilitation *in vitro*

Neira Polet Camacho-Hernández, Jonathan Julio Lorea-Hernández, Fernando Peña-Ortega*

Departamento de Neurobiología del Desarrollo y Neurofisiología, Instituto de Neurobiología, Universidad Nacional Autónoma de México, Querétaro, Qro, 76230, Mexico

ARTICLE INFO

Keywords:
Respiratory plasticity
Glia
Hypoxia
preBötzinger complex
Inflammation

ABSTRACT

Inflammation inhibits the expression of some, but not all forms of respiratory motor plasticity. For example, systemic application of lipopolysaccharide (LPS) inhibits the phrenic long-term facilitation induced by moderate-intermittent hypoxia *in vivo*. There are multiple pro-inflammatory processes triggered by the systemic application of LPS, including neuroinflammation in the CNS. Considering that microglia can be activated by the systemic application of LPS, it is likely that this cell type influences the response of the respiratory circuits to intermittent hypoxia (IH). Thus, we aimed to test whether modulators of microglial function would affect the response to IH of the preBötzinger complex (preBötC) isolated in a brainstem slice preparation. This experimental approach avoids the systemic influences of these microglial modulators and limits their effects on cells, mostly microglia, included in the slice. First, we found that IH (3 × 5-min episodes of bubbling with 95% N_2 and 5% CO_2, mixed with 5-min normoxic intervals by bubbling with 95% O_2 and 5% CO_2) induces a long-lasting increase in the respiratory rhythm frequency recorded directly from the preBötC, called *in vitro* long-term facilitation (LTF), which occurs simultaneously with a long-lasting decrease in burst amplitude. Moreover, we found that bath applications of "microglial activators" (LPS and fractalkine), "microglial inhibitors" (minocycline and fucoidan) and a microgliotoxin (liposomal clodronate) partially reduce *in vitro* LTF. These findings reveal a complex scenario in which both the activation and the inhibition of microglia halts IH-induced preBötC plasticity and suggest that experimental or pathological conditions that affect this cell type, almost in any way, could affect breathing and its plastic responses.

1. Introduction

Inflammation associated with a variety of pathological conditions affects neural functions, including breathing generation and control (Herlenius, 2011; Lu et al., 2012; Tadmouri et al., 2014; Lorea-Hernández et al., 2016; Stokes et al., 2017). Inflammation also affects respiratory adaptations to physiological challenges (Tadmouri et al., 2014; Stokes et al., 2017) and the respiratory plasticity that results from some of them (Vinit et al., 2011; Huxtable et al., 2011, 2013; 2015; 2018; Agosto-Marlin et al., 2017). One respiratory plastic phenomenon that is affected by inflammation is phrenic long-term facilitation (pLTF), which consists of a long-lasting increase in the respiratory phrenic motor output following acute intermittent hypoxia (IH; Vinit et al., 2011; Huxtable et al., 2011, 2013; 2018; Agosto-Marlin et al., 2017). Phrenic LTF is a highly complex phenomenon that includes changes in burst frequency or amplitude (or both), mainly produced by plastic changes at the motoneuron level (MacFarlane et al., 2008, 2009; Navarrete-Opazo and Mitchell, 2014), and which can be dependent on either adenosinergic or serotonergic modulation (MacFarlane et al., 2008, 2009; Navarrete-Opazo and Mitchell, 2014; Agosto-Marlin et al., 2017). IH is a feature of pathological conditions such as those encountered during sleep apneas (MacFarlane et al., 2008, 2009; Navarrete-Opazo and Mitchell, 2014), but it can also be used as a therapeutic approach to treat neurological dysfunctions when applied in a moderate and controlled regime (Dale et al., 2014; Gonzalez-Rothi et al., 1985). Interestingly, systemic inflammation elicited by lipopolysaccharide (LPS) (Vinit et al., 2011; Huxtable et al., 2011, 2013; 2018; Agosto-Marlin et al., 2017) or several hours of IH (Huxtable et al., 2015; 2018) abolishes serotonin-dependent pLTF. Despite the fact that some cellular mechanisms related to this inhibition have started to emerge (Huxtable et al., 2011, 2013; 2018; MacFarlane et al., 2014), the cell types involved in this inhibition have yet to be revealed. It is likely that microglia can modulate LTF generation, since systemic inflammation can activate microglial cells in the central nervous system

* Corresponding author at: Departamento de Neurobiología del Desarrollo y Neurofisiología, Instituto de Neurobiología, Universidad Nacional Autónoma de México, Boulevard Juriquilla 3001, Juriquilla, Querétaro, QRO, CP 76230, Mexico.
E-mail address: jfpena@unam.mx (F. Peña-Ortega).

https://doi.org/10.1016/j.resp.2018.07.012
Received 11 February 2018; Received in revised form 8 June 2018; Accepted 30 July 2018
Available online 31 July 2018

(CNS), specifically in the brainstem (Huxtable et al., 2011; Tadmouri et al., 2014; Stokes et al., 2017). The "microglial inhibitor" minocycline (Peña-Ortega, 2017) affects pLTF (Huxtable et al., 2011), and microglia modulates respiratory rhythm generation *in vitro* (Lu et al., 2012; Lorea-Hernández et al., 2016).

As mentioned, peripheral inflammation can induce central neuroinflammation (Elmore et al., 2014; Henry et al., 2009; Liu et al., 2012), which is a phenomenon partially mediated by microglial activation (Elmore et al., 2014; Henry et al., 2009; Liu et al., 2012). Microglial activation is a complex and dynamic phenomenon that renders microglia in a variety of phenotypes that are not entirely described by the classic M1 and M2 phenotypes and that can coexist in place and time (Cherry et al., 2014; Shigemoto-Mogami et al., 2014; Peña-Ortega, 2017). Peripheral inflammation can be translated into the CNS by inflammatory molecules crossing the blood-brain barrier into the CNS *via* active transport (Banks et al., 1991, 1994) or *via* circumventricular regions that lack an effective blood-brain barrier (Wuchert et al., 2008, 2009). Circulating cytokines also bind to brain endothelial cells and induce the production of proinflammatory molecules such as nitric oxide (NO) or prostaglandins that cross the blood–brain barrier or increase blood–brain barrier permeability (Ek et al., 2001; Engblom et al., 2002; Herlenius, 2011). Peripheral inflammation can also be transmitted to the CNS through vagus nerve activation (Ek et al., 1998; Goehler et al., 2005; Balan et al., 2011). For instance, peripheral IL-1β or LPS elicits brainstem inflammation (Johnson et al., 2018), which is abolished by bilateral vagotomy (Layé et al., 1995; Bluthé et al., 1996). Altogether, this evidence indicates that peripheral inflammation induced by LPS or several hours of IH could induce neuroinflammation, and perhaps contribute to pLTF inhibition (Vinit et al., 2011; Huxtable et al., 2011, 2013; 2015; 2018).

Some plastic changes that may be related to pLTF can be reproduced in the brainstem slice preparation containing the preBötzinger complex (preBötC) by applying IH *in vitro* while directly recording preBötC-generated respiratory rhythm in a brainstem slice (Blitz and Ramirez, 2002). This preparation allows for the direct evaluation of the influence of CNS cell-types on the preBötC, without the "contamination" of the effects that peripheral immune cells would have in more intact preparations (Lu et al., 2012; Lorea-Hernández et al., 2016). Considering that the pro-inflammatory processes triggered by the systemic application of LPS are multifaceted and might include changes in the CNS and, furthermore, considering that microglia can be activated by the systemic inflammation induced by either LPS or IH, or by their direct application to microglia (Pardo-Peña et al., 2018), we hypothesized that microglia might influence the response of the respiratory circuits to IH. Thus, here we aimed to characterize the effects of several modulators of microglial function on the changes induced by IH in the activity of the preBötC isolated in a brainstem slice preparation, avoiding the systemic effects of these modulators and limiting their actions to cells, mostly microglia, included in this isolated preparation. Thus, we tested the effects of modulators of microglial function, including "activators", "inhibitors" or a microgliotoxin (Peña-Ortega, 2017) on IH-induced changes in preBötC activity. We found that IH induces a long-lasting change in preBötC activity that is reduced by all microglial modulators tested, suggesting that microglia modulate *in vitro* LTF and that experimental or pathological conditions that affect this cell type, almost in any way, could affect respiratory plasticity.

2. Experimental procedures

2.1. Ethics statement

The Bioethics Committee of the Institute of Neurobiology at Universidad Nacional Autónoma de México approved all experimental procedures, which were carried out in accordance with the guidelines of the Institutional Animal Care and Use Committee Guidebook (NIH publication 80-23, Bethesda, MD, USA, 1996).

2.2. Brainstem slice preparation

Details of the slice preparation have been previously reported (Peña et al., 2004, 2008). Briefly, 6- to 8-day old male or female CD-1 mice were anesthetized and decapitated, and brainstems were removed and placed in ice-cold artificial cerebrospinal fluid (ACSF) bubbled with carbogen (95% O_2 and 5% CO_2). The ACSF (pH 7.4) contained (in mM): 119 NaCl, 3 KCl, 1.5 $CaCl_2$, 1 $MgCl_2$, 25 $NaHCO_3$ and 30 D-glucose. Brainstems were mounted on a vibratome (The Vibratome Company, St. Louis, MO) and serially sliced until the rostral boundary of the preBötC was identified. A single slice (700 µm thick) per animal was obtained and transferred into a perfusion chamber. Thus, each experimental condition was tested in a set of preparations consisting of independent slices obtained from different animals. Each slice was perfused by recirculating 30 ml of ACSF bubbled with carbogen at a flow rate of 20 ml/min (Peña et al., 2004, 2008). The temperature was maintained at 29 ± 1 °C. Extracellular KCl was elevated from 3 mM to 8 mM over a span of 30 min before starting the recordings (Tryba et al., 2003). Hypoxic conditions were induced by removing carbogen and bubbling the ACSF with a nitrogenous gas mixture (95% N_2 and 5% CO_2). IH consisted of three periods of hypoxia (5 min) mixed with periods of carbogen bubbling (5 min) (Blitz and Ramirez, 2002). After IH, reoxygenation was achieved by bubbling the ACSF with carbogen again for at least 60 min (Peña et al., 2004, 2008). IH was applied only to slices that showed a stable rhythm for at least 30 min; this was considered "basal activity" or "pre-IH". All drugs were bath applied and left in the bath for at least one hour before any experimental manipulation, with the exception of the microglial toxin liposomal clodronate (140 µg/ml; n = 8; Kumamaru et al., 2012; Lorea-Hernández et al., 2016), which was bath applied for at least 120 min before any experimental manipulation. We used the putative microglial activators lipopolysaccharide 200 ng/ml (LPS, from *Escherichia Coli*, Sigma-Aldrich; n = 8; Mayer et al., 2014; Lorea-Hernández et al., 2016; Peña-Ortega, 2017) and fractalkine 1 µg/ml (Biolegend, San Diego, CA; n = 8; Sun et al., 2015; Lorea-Hernández et al., 2016; Peña-Ortega, 2017), the putative microglial inhibitors minocycline 30 µM (Minocycline hydrochloride, Sigma-Aldrich; n = 10; Matsukawa et al., 2009; Lorea-Hernández et al., 2016; Peña-Ortega, 2017) and fucoidan 5 µg/ml (FCD, Sigma-Aldrich; n = 8; Do et al., 2010; Lorea-Hernández et al., 2016; Peña-Ortega, 2017).

Liposomal clodronate was obtained by encapsulating clodronate (Dichloromethylenediphosphonic acid disodium salt, Sigma-Aldrich) in liposomes as previously described (van Rooijen and Sanders, 1996; Pardo-Peña et al., 2018). Briefly, phosphatidylcholine 86 mg and cholesterol 8 mg were dissolved in chloroform 10 ml and poured into a round-bottom flask located in a roto-evaporator to separate the chloroform from the lipids. The thin film that formed inside the flask after high-vacuum rotary evaporation was dispersed in 10 ml of clodronate dissolved in distilled water at 0.6 M. To avoid lipid oxidation, this solution was bubbled with nitrogen for 2 h. Non-encapsulated clodronate was removed by centrifugation at 12,000 rpm for 15 min. The supernatant was removed, and the pellet was re-suspended in sterile potassium buffer solution (PBS). This last procedure was repeated three times with centrifugation lasting 30 min. The last suspension containing liposomal clodronate in PBS was stored at 4 °C for final use in a period not exceeding 2 weeks (van Rooijen and Sander 1996; Pardo-Peña et al., 2018).

2.3. Electrophysiological recordings

Population activity of the preBötC was recorded with glass suction electrodes positioned on the surface of the slice at the level of the preBötC (Peña et al., 2004, 2008). The signal was amplified and filtered (low pass, 0.25 KHz; high pass, 5 Hz) using a wide-band AC amplifier (Grass Instruments, Quincy, MA). The signal was also rectified and integrated by using an electronic filter (time constant of 30–50 ms;

designed by JFI electronics at The University of Chicago) (Zavala-Tecuapetla et al., 2008; 2014). The experimental protocol consisted of 30 min of basal recording, followed by the IH protocol described before (Blitz and Ramirez, 2002) with a reoxygenation period of at least 60 min.

2.4. Data analysis and statistics

Signals were digitalized at 5000 Hz using an analog-to-digital converter (BNC-2110, National Instruments) and stored on a personal computer for offline analysis. Signal amplitude was expressed in arbitrary units (a.u.). To calculate the irregularity score we used the following formula: $S_n = ABS (P_n - P_{n-1})/P_{n-1}$, where S_n is the score of the *n*th cycle, P_n represents its period, P_n-1 is the period of the preceding burst, and ABS is the absolute value. We calculated the coefficient of variation (CV) of the amplitude and frequency as follows: CV = (standard deviation/mean) (Ramírez-Jarquín et al., 2012). Recordings were analyzed using IGOR-Pro (WaveMetrics, Lake Oswego, OR). Data were normalized to pre-IH conditions (defined as 100%) in most cases and to basal activity for the non-treated slices left unperturbed. The results are expressed as the mean ± SEM and comparisons were drawn using the Kruskal-Wallis test followed by Dunn's test when comparing several experimental groups. When comparing two groups, the Mann-Whitney U test was used. When comparing quantifications within the same group, the Wilcoxon test was used. For the data presented in graphs, statistical comparisions were performed on the normalized data. For the data presented in Table 1, statistical comparisions were performed on the non-normalized data. We used non-parametric statistics because our data lacked normal/Gaussian distribution and our sample sizes were small (between 8 and 10). Statistical analyses were performed using GraphPad Prism (version 5.0), and differences were considered significant with $p < 0.05$.

3. Results

3.1. Acute intermittent hypoxia induces long-term facilitation in vitro

The fictive respiratory rhythm recorded from the preBötC in control slices (in the absence of any drug) showed a frequency of 0.43 ± 0.09 Hz and an amplitude of 1.52 ± 0.19 a.u. under basal conditions (n = 17; Fig. 1). To test the stability of this activity under *in vitro* conditions, a subgroup of non-treated slices was left unperturbed in the chamber while recording their activity for two hours (n = 7). The basal respiratory rhythm frequency of these slices was 0.32 ± 0.05 Hz (irregularity (IR) of 0.32 ± 0.04 and variation coefficient (CV) of 0.24 ± 0.03, Table 1) and their burst amplitude was 1.82 ± 0.20 a.u. (CV of 0.14 ± 0.02, Table 1). These values remained unchanged after two hours of continuous recording, as the slices exhibited a respiratory rhythm frequency of 0.33 ± 0.05 Hz (104.87 ± 5.44% of basal; n = 7; $p < 0.05$, Fig. 1A) and a burst amplitude of 1.79 ± 0.22 a.u. (97.29 ± 2.99% of basal; n = 7; $p < 0.05$, Fig. 1A), which is not different from the variables quantified at the beginning of the experiments ($p > 0.05$). The variability measurements (IR and CV) did not change after two hours either ($p > 0.05$; n = 7; Fig. 1A). For comparison purposes, these long-term quantifications will be referred to as "control" for the rest of the experiments.

To corroborate that IH induces LTF *in vitro* (Blitz and Ramirez, 2002), an independent group of non-treated slices, with a basal respiratory rhythm frequency of 0.50 ± 0.09 Hz (CV of 0.26 ± 0.03 and IR of 0.32 ± 0.04; n = 10; Table 1) and a burst amplitude of 1.30 ± 0.11 a.u. (CV of 0.16 ± 0.02; n = 10; Table 1), were treated with IH, which induces a long-lasting change in respiratory rhythm characterized by an increase in respiratory rhythm frequency. This frequency reaches statistical significance starting at 5 min after IH (148.66 ± 14.41% of basal; n = 10; $p < 0.05$, Fig. 1B). The increase in respiratory rhythm frequency occurs simultaneously with a decrease in burst amplitude, which reaches statistical significance starting at

Table 1
Parameters of the respiratory rhythm generated under the different experimental conditions tested in this study.

Condition	Amplitude (a.u.)	Amplitude CV	Frequency (Hz)	Frequency CV	Frequency Irregularity
		Basal activity			
Control (n = 7)	1.82 ± 0.20	0.14 ± 0.02	0.32 ± 0.05	0.24 ± 0.03	0.32 ± 0.04
IH (n = 10)	1.30 ± 0.11	0.16 ± 0.02	0.50 ± 0.09	0.26 ± 0.03	0.32 ± 0.05
LPS (n = 8)	2.09 ± 0.25	0.10 ± 0.01	0.27 ± 0.05	0.31 ± 0.04	0.33 ± 0.05
FKN (n = 8)	2.00 ± 0.18	0.10 ± 0.01	0.34 ± 0.05	0.25 ± 0.03	0.29 ± 0.03
MIN (n = 10)	1.81 ± 0.14	0.16 ± 0.02	0.27 ± 0.07	0.25 ± 0.04	0.32 ± 0.06
FCD (n = 8)	1.54 ± 0.21	0.18 ± 0.02	0.51 ± 0.07	0.41 ± 0.10	0.43 ± 0.08
Lip-Clo (8)	1.94 ± 0.19	0.13 ± 0.02	0.36 ± 0.05	0.23 ± 0.03	0.27 ± 0.03
		After treatment			
Control (n = 7)	1.79 ± 0.22	0.15 ± 0.01	0.33 ± 0.05	0.51 ± 0.20	0.36 ± 0.04
IH (n = 10)					
LPS (n = 8)	1.69 ± 0.24	0.19 ± 0.04	0.33 ± 0.02	0.25 ± 0.01	0.35 ± 0.02
FKN (n = 8)	1.73 ± 0.18	0.14 ± 0.02	0.40 ± 0.06	0.28 ± 0.03	0.35 ± 0.06
MIN (n = 10)	1.54 ± 0.18	0.18 ± 0.02	0.36 ± 0.08	0.35 ± 0.05	0.44 ± 0.07
FCD (n = 8)	1.36 ± 0.19	0.18 ± 0.02	**0.58 ± 0.08**	0.47 ± 0.07	0.49 ± 0.09
Lip-Clo (8)	1.46 ± 0.18	0.17 ± 0.02	0.47 ± 0.07	0.27 ± 0.06	0.29 ± 0.06
		60 min after intermittent hypoxia			
Control (n = 7)					
IH (n = 10)	**0.94 ± 0.08**	0.20 ± 0.03	**0.77 ± 0.08**	0.40 ± 0.06	0.53 ± 0.09
LPS (n = 8)	*1.57 ± 0.21*	0.21 ± 0.03	*0.41 ± 0.02*	0.29 ± 0.02	0.35 ± 0.04
FKN (n = 8)	*1.31 ± 0.14*	0.16 ± 0.02	*0.47 ± 0.08*	*0.24 ± 0.03*	*0.30 ± 0.03*
MIN (n = 10)	*1.44 ± 0.22*	0.20 ± 0.03	*0.46 ± 0.09*	0.42 ± 0.07	0.63 ± 0.17
FCD (n = 8)	**1.24 ± 0.16**	0.20 ± 0.02	**0.65 ± 0.07**	0.58 ± 0.09	**0.59 ± 0.09**
Lip-Clo (8)	*1.37 ± 0.19*	0.16 ± 0.01	***0.49 ± 0.05***	0.29 ± 0.04	0.36 ± 0.06

a.u. Arbitrary units; CV, coefficient of variation; IH, intermittent hypoxia; LPS, lipopolysaccharide; FKN, fractalkine; MIN, minocycline; FCD, fucoidan; Lip-Clo, liposomal clodronate. Underlined numbers denote a significantly difference vs previous condition; bold numbers denote a significantly difference vs control group; numbers in italics denote a significantly difference vs IH group ($p < 0.05$ for the non-normalized data included in the Table).

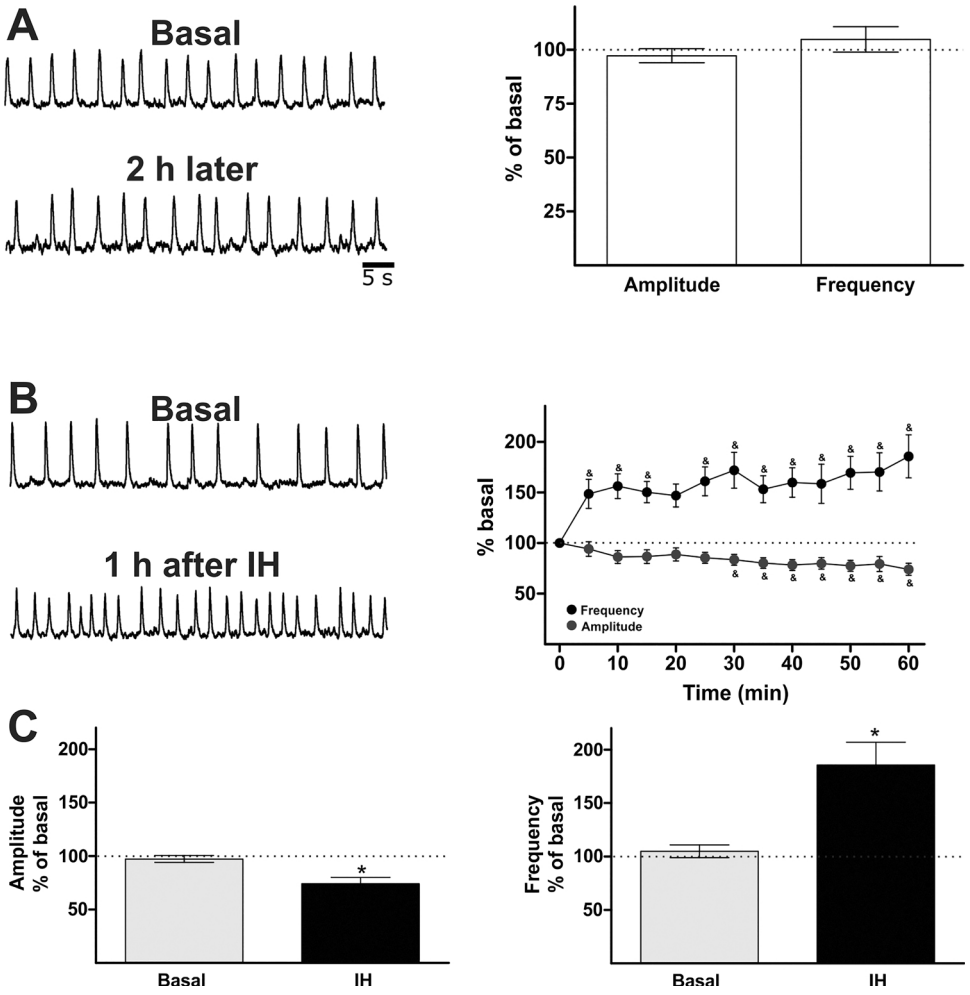

Fig. 1. Temporal stability of the respiratory rhythm and its long-term response to intermittent hypoxia *in vitro*. (A) On the left, representative recordings of the respiratory rhythm generated in a brainstem slice at the start (upper trace; basal) and end of a 2-h recording (lower trace). On the right, the quantification of respiratory rhythm frequency and amplitude 2 h after starting the recordings are show as % of basal (set as 100%; n = 7). (B) On the left, representative recordings of the respiratory rhythm generated in a brainstem slice under control conditions (upper trace; basal) and 1 h after the application of intermittent hypoxia (IH). On the right, the time-course of the change in respiratory rhythm frequency (black dots) and amplitude (gray dots) after IH is shown (n = 10). (C) The quantification of respiratory rhythm frequency (right graph) and amplitude (left graph) 1 h after IH is shown as % of basal (set as 100%; n = 10). * denotes a significant difference compared to the control group (slices not treated with IH; *i.e.*, those in panel A), & denotes a significant difference compared to its own basal activity ($p < 0.05$ for normalized data).

30 min after IH (83.58 ± 5.34% of basal; n = 10; $p < 0.05$ *vs* control, Fig. 1B). One hour after the application of IH, respiratory rhythm frequency increased to 0.77 ± 0.08 Hz (185.65 ± 20.15% of basal; n = 10; $p < 0.05$ *vs* control, Fig. 1). Respiratory rhythm frequency variability also significantly increased one hour after IH (CV of 0.40 ± 0.06; $p < 0.05$ *vs* control; n = 10; Table 1). One hour after the application of IH, burst amplitude decreased to 0.94 ± 0.08 a.u. (74.16 ± 5.63% of basal; n = 10; $p < 0.05$ *vs* control, Fig. 1). Burst amplitude variability significantly increased one hour after IH (CV of 0.20 ± 0.03; $p < 0.05$; n = 10; Table 1). The long-lasting increase in respiratory rhythm frequency after IH coincides with the LTF reported by Blitz and Ramirez (2002) under similar experimental conditions. For comparison purposes, these quantifications will be referred to as "control IH" for the rest of the experiments.

3.2. Microglial activators partially inhibit long-term facilitation in vitro

To evaluate whether common pharmacological tools used to activate microglia (Peña-Ortega, 2017) could modulate *in vitro* LTF, we pre-treated slices with either LPS or fractalkine and recorded their long-lasting response to IH *in vitro*. The fictive respiratory rhythm recorded from the preBötC in slices pre-treated with LPS showed a frequency of 0.33 ± 0.02 Hz and an amplitude of 1.69 ± 0.24 a.u. under normoxic conditions before IH (basal; n = 8; Fig. 2). While burst frequency tends to be faster than the one recorded in the absence of LPS (0.27 ± 0.05 Hz, $p = 0.08$; n = 8; Table 1), burst amplitude was significantly smaller than the one recorded in the absence of LPS (2.09 ± 0.25 a.u., $p < 0.05$; n = 8; Table 1), as previously reported (Lorea-Hernández et al., 2016). The burst amplitude CV increased in the presence of LPS (from 0.10 ± 0.01 to 0.19 ± 0.04; n = 8; Table 1). Application of IH to these slices induced an increase in respiratory rhythm frequency with no change in burst amplitude when compared to control slices. In LPS pre-treated slices, respiratory rhythm frequency increased to 0.41 ± 0.02 Hz one hour after the application of IH (132.11 ± 7.53% of basal; n = 8; $p < 0.05$ *vs* control, Fig. 2). Burst amplitude remained unchanged after IH at 1.57 ± 0.21 Hz (97.76 ± 9.41% of basal; n = 8; $p > 0.05$ *vs* control, Fig. 2). The variability of burst amplitude and frequency did not change after IH in this group (Table 1; n = 8; $p > 0.05$). Although LPS pre-treated slices exhibited *in vitro* LTF, this long-lasting increase in respiratory rhythm frequency tends to be smaller than the one observed in non-pre-treated slices when normalized data are tested ($p = 0.0506$ *vs* control IH; n = 8; Fig. 2) but is significantly smaller when non-normalized data are tested ($p < 0.05$ vs control IH; Table 1). Moreover, the burst amplitude observed in LPS pre-treated slices is significantly larger than the one observed in control slices after IH ($p < 0.05$ *vs* control IH; n = 8; Fig. 2).

The fictive respiratory rhythm recorded from the preBötC in slices pre-treated with fractalkine showed a frequency of 0.40 ± 0.06 Hz and an amplitude of 1.73 ± 0.18 a.u. under normoxic conditions before IH (basal; n = 8; Fig. 2). While burst frequency remained unchanged compared to the one recorded in the absence of fractalkine (0.34 ± 0.05 Hz; n = 8; $p > 0.05$, Table 1), burst amplitude was significantly smaller than the one recorded in the absence of fractalkine (2.00 ± 0.18 a.u.; n = 8; $p < 0.05$, Table 1) as previously reported (Lorea-Hernández et al., 2016). The variability of burst and frequency did not change in the presence of fractalkine (n = 8; Table 1). Application of IH induced a decrease in the respiratory rhythm burst

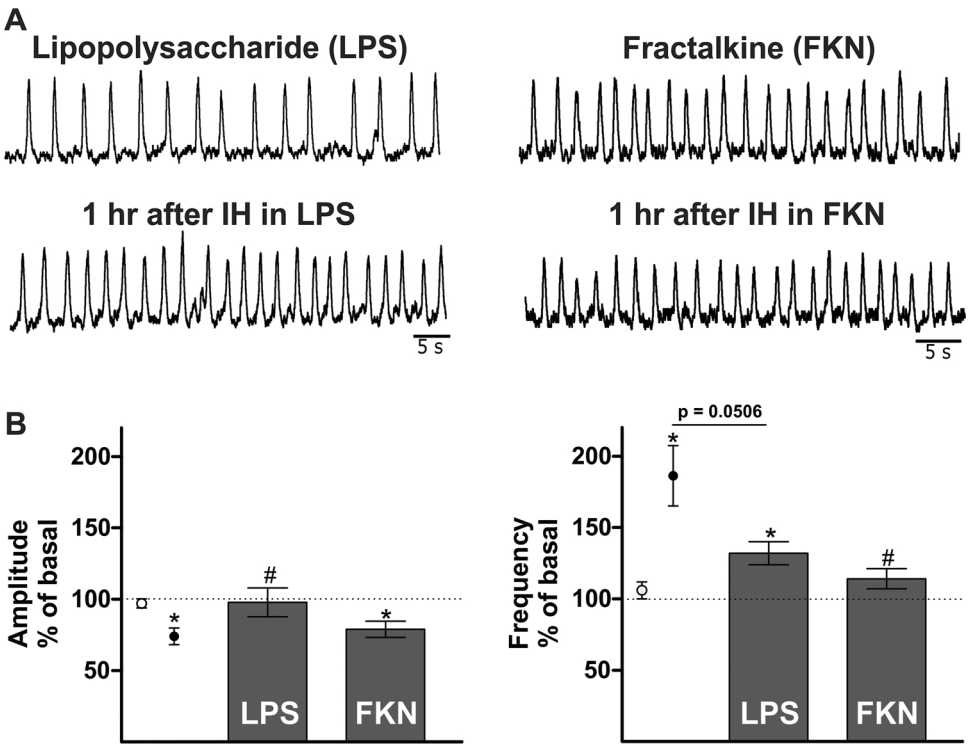

Fig. 2. Microglial activators partially block the long-term change in respiratory rhythm induced by intermittent hypoxia *in vitro*. (A) On the left, representative recordings of the respiratory rhythm generated in a brainstem slice in the presence of lipopolysaccharide (LPS; upper trace; basal) and 1 h after the application of intermittent hypoxia (IH) in the continuous presence of LPS (lower trace). On the right, representative recordings of the respiratory rhythm generated in a brainstem slice in the presence of fractalkine (FKN; upper trace; basal) and 1 h after the application of intermittent hypoxia (IH) in the continuous presence of FKN (lower trace). (B) The quantification of respiratory rhythm frequency (right graph) and amplitude (left graph) 1 h after IH is shown as % of basal (set as 100%; n = 8 in both cases). The corresponding quantifications of each variable are included as a white dot for the control group and as a black dot for the IH control group. * denotes a significant difference compared to the control group ($p < 0.05$ for normalized data). # denotes a significant difference compared to the IH control group ($p < 0.05$ for normalized data). The p value for the comparison between the normalized of the IH control group *vs* the LPS group is also shown.

amplitude with no change in its frequency when compared to control slices. In fractalkine pre-treated slices, respiratory rhythm frequency remained unchanged one hour after the application of IH, when compared to control slices, at 0.47 ± 0.08 Hz (114.21 ± 6.54% of basal; n = 8; $p > 0.05$ *vs* control, Fig. 2). However, this frequency is significantly higher than the one observed in the same slices before IH ($p < 0.05$ *vs* own basal; n = 8). In fractalkine pre-treated slices, burst amplitude was reduced to 1.31 ± 0.14 a.u. one hour after the application of IH (78.89 ± 5.29% of basal; n = 8; $p < 0.05$ *vs* control, Fig. 2). The variability of burst amplitude and frequency did not change after IH in this group (Table 1; n = 8; $p > 0.05$). However, the variability of burst frequency in these slices was smaller than the one observed in non-pre-treated slices after IH (Table 1; n = 8; $p < 0.05$ vs control IH). Even though fractalkine pre-treated slices exhibited a slight long-lasting increase in respiratory rhythm frequency after IH, this increase is significantly smaller than the one observed in non-pre-treated slices ($p < 0.05$ *vs* control IH; n = 8; Fig. 2). The decrease in burst amplitude after IH was similar to the one observed in non-pre-treated slices ($p > 0.05$ *vs* control IH; n = 8; Fig. 2).

3.3. Microglial inhibitors partially inhibit long-term facilitation in vitro

To evaluate whether pharmacological tools used to inhibit microglia (Peña-Ortega, 2017) could modulate *in vitro* LTF, we pre-treated slices with either minocycline or fucoidan and recorded their long-lasting response to IH *in vitro*. The fictive respiratory rhythm recorded from the preBötC in slices pre-treated with minocycline showed a frequency of 0.36 ± 0.08 Hz and an amplitude of 1.54 ± 0.18 a.u. under normoxic conditions before IH (basal; n = 10; Fig. 3). Respiratory rhythm frequency was faster than the one recorded in the absence of minocycline (0.27 ± 0.07 Hz; n = 10; $p < 0.05$, Table 1). Burst amplitude after application of minocycline was significantly smaller than the one recorded in the absence of the drug (1.81 ± 0.14 a.u.; n = 10; $p < 0.05$, Table 1) as previously reported (Lorea-Hernández et al., 2016). The variability of burst amplitude and frequency did not change in the presence of minocycline (Table 1; n = 10; $p > 0.05$). Application of IH to these slices induced an increase in respiratory rhythm frequency with no change in burst amplitude when compared to control slices. In minocycline pre-treated slices, respiratory rhythm frequency increased to 0.46 ± 0.09 Hz one hour after the application of IH (134.32 ± 9.24% of basal; n = 10; $p < 0.05$ *vs* control, Fig. 3), whereas burst amplitude remained unchanged, when compared to control slices, at 1.44 ± 0.22 Hz (90.79 ± 5.71% of basal; n = 10; $p > 0.05$ *vs* control, Fig. 3). However, this amplitude tended to be smaller than the one observed in the same slices before IH (n = 10; $p = 0.0801$). The variability of burst amplitude and frequency did not change after IH in this group (Table 1; n = 10; $p > 0.05$). Despite the fact that minocycline pre-treated slices exhibited *in vitro* LTF, this long-lasting increase in respiratory rhythm frequency is smaller than the one observed in non-pre-treated slices ($p < 0.05$ *vs* control IH; n = 10; Fig. 3). Moreover, the burst amplitude observed in minocycline pre-treated slices is significantly larger than the one observed in control slices after IH ($p < 0.05$ *vs* control IH; n = 10; Fig. 2).

The fictive respiratory rhythm recorded from the preBötC in slices pre-treated with fucoidan showed a frequency of 0.58 ± 0.08 Hz and an amplitude of 1.36 ± 0.19 a.u. under normoxic conditions before IH (basal; n = 8; Fig. 3). While burst frequency tended to be faster than the one recorded in the absence of fucoidan (0.51 ± 0.07 Hz; n = 8; $p = 0.06$, Table 1), burst amplitude was significantly smaller than the one recorded in the absence of fucoidan (1.54 ± 0.21 a.u.; n = 8; $p < 0.05$, Table 1) as previously reported (Lorea-Hernández et al., 2016). The variability of burst amplitude and frequency did not change in the presence of fucoidan (Table 1; n = 8; $p > 0.05$). Application of IH induced no major changes in frequency or amplitude of the respiratory rhythm when compared to control slices. In fucoidan pre-treated slices, respiratory rhythm frequency remained unchanged one hour after the application of IH, when compared to control slices, at 0.65 ± 0.07 Hz (115.21 ± 5.84% of basal; n = 8; $p > 0.05$ *vs* control, Fig. 3). However, this frequency is significantly higher than the one observed in the same slices before IH ($p < 0.05$ *vs* own basal; n = 8). In fucoidan pre-treated slices, burst amplitude remained unchanged at 1.24 ± 0.16 a.u. one hour after the application of IH (99.48 ± 15.98% of basal; n = 8; $p > 0.05$ *vs* control, Fig. 3). Respiratory rhythm frequency after IH in fucoidan-treated slices was

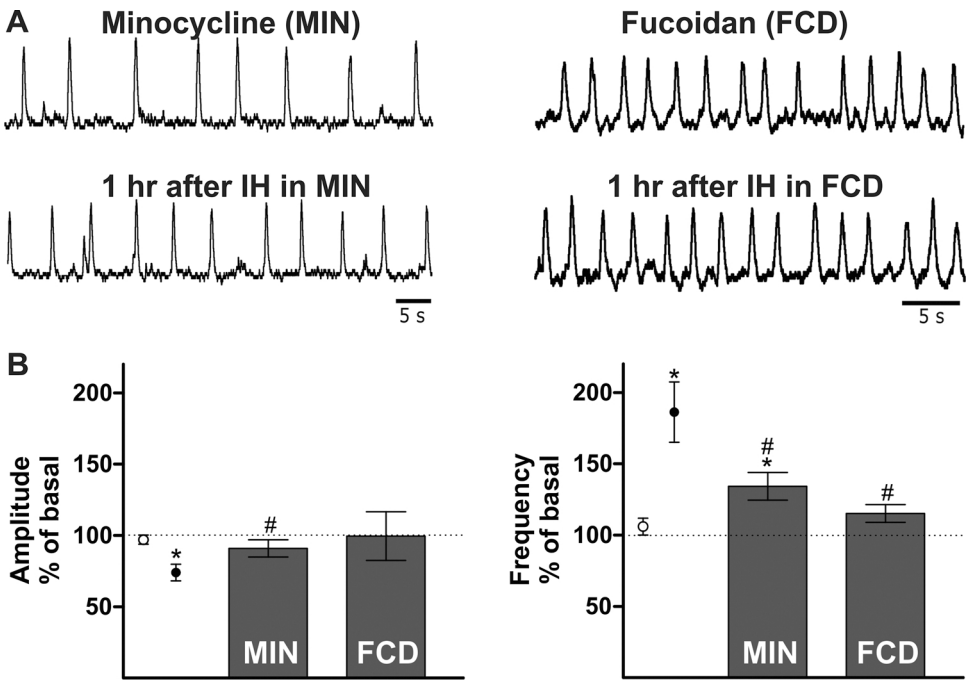

Fig. 3. Microglial inhibitors partially block the long-term change in respiratory rhythm induced by intermittent hypoxia *in vitro*. (A) On the left, representative recordings of the respiratory rhythm generated in a brainstem slice in the presence of minocycline (MIN; upper trace; basal) and 1 h after the application of intermittent hypoxia (IH) in the continuous presence of MIN (lower trace). On the right, representative recordings of the respiratory rhythm generated in a brainstem slice in the presence of fucoidan (FCD; upper trace; basal) and 1 h after the application of IH in the continuous presence of FCD (lower trace). (B) The quantification of the respiratory rhythm frequency (right graph) and amplitude (left graph) 1 h after IH is shown as % of basal (set as 100%; n = 8 for FCD and n = 10 for MIN). The corresponding quantifications of each variable are included as a white dot for the control group and as a black dot for the IH control group. * denotes a significant difference compared to the control group ($p < 0.05$ for normalized data). # denotes a significant difference compared to the IH control group ($p < 0.05$ for normalized data).

significantly lower than the one observed in non-pre-treated slices ($p < 0.05$ *vs* control IH; n = 8; Fig. 3), although burst amplitude was similar to the one observed in non-pre-treated slices ($p > 0.05$ *vs* control IH; n = 8; Fig. 3). The irregularity of respiratory rhythm frequency increased after IH in the presence of fucoidan (Table 1; n = 8; $p < 0.05$), while variability of burst amplitude did not change after IH in this group (Table 1; n = 8; $p > 0.05$).

3.4. The microglia toxin liposomal clodronate partially blocks long-term facilitationin vitro

To further support that microglia modulate *in vitro* LTF, we tested whether liposomal clodronate, a microglial toxin (Peña-Ortega, 2017), could modulate this plastic phenomenon. The fictive respiratory rhythm recorded from the preBötC in slices pre-treated with liposomal clodronate showed a frequency of 0.47 ± 0.07 Hz and an amplitude of 1.46 ± 0.18 a.u. under normoxic conditions before IH (basal; n = 8; Fig. 4). Respiratory rhythm frequency became faster than the one recorded in the absence of liposomal clodronate (0.36 ± 0.05 Hz; n = 8; $p < 0.05$, Table 1). The burst amplitude recorded in the presence of liposomal clodronate was smaller than the one recorded in the absence of the microgliotoxin (1.94 ± 0.19 a.u.; n = 8; $p < 0.05$, Table 1) as previously reported (Lorea-Hernández et al., 2016). The burst amplitude CV increase in the presence of liposomal clodronate (from 0.13 ± 0.02 to 0.17 ± 0.02; n = 8; Table 1). Application of IH did not induce major changes in frequency or amplitude of the respiratory rhythm, compared to control slices. In slices pre-treated with liposomal clodronate, one hour after IH application, the respiratory rhythm frequency remained at 0.49 ± 0.05 Hz (109.57 ± 4.40% of basal; n = 8; $p < 0.05$ *vs* control, Fig. 4), whereas the burst amplitude also remained unchanged, when compared to control slices, at 1.37 ± 0.19 a.u. (87.58 ± 4.87% of basal; n = 8; $p < 0.05$ *vs* control, Fig. 4). However, this amplitude is significantly smaller than the one observed in the same slices before IH ($p < 0.05$ *vs* own basal; n = 8). The respiratory rhythm frequency after IH in slices pre-treated with liposomal clodronate is significantly lower than the one observed in non-pre-treated slices ($p < 0.05$ *vs* control IH; n = 8; Fig. 4), whereas the burst amplitude was significantly higher than the one observed in non-pre-

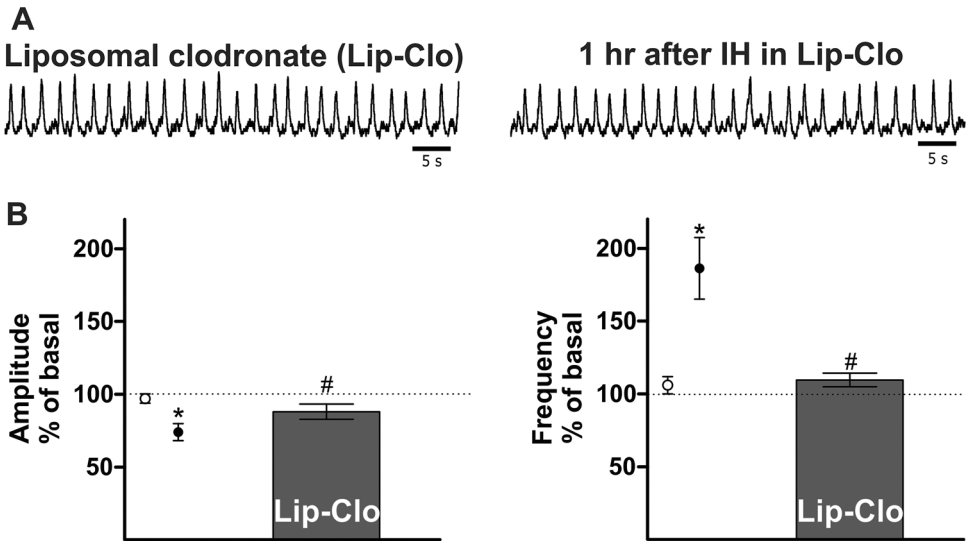

Fig. 4. The microgliotoxin liposomal clodronate blocks the long-term change in respiratory rhythm induced by intermittent hypoxia *in vitro*. (A) Representative recordings of the respiratory rhythm generated in a brainstem slice in the presence of liposomal clodronate (Lip-Clo; left trace; basal) and 1 h after the application of intermittent hypoxia (IH) in the continuous presence of Lip-Clo (right trace). (B) The quantification of the respiratory rhythm frequency (right graph) and amplitude (left graph) 1 h after IH is shown as % of basal (set as 100%; n = 8). The corresponding quantifications of each variable are included as a white dot for the control group and as a black dot for the IH control group. * denotes a significant difference compared to the control group ($p < 0.05$ for normalized data). # denotes a significant difference compared to the IH control group ($p < 0.05$ for normalized data).

treated slices ($p < 0.05$ *vs* control IH; n = 8; Fig. 4). The irregularity of respiratory rhythm frequency increased after IH in the presence of liposomal clodronate (Table 1; n = 8; $p < 0.05$), while variability of burst amplitude did not change after IH in this group (Table 1; n = 8; $p > 0.05$).

4. Discussion

Our results show that *in vitro* LTF induced upon IH application to brainstem slices containing preBötC is highly susceptible to pharmacological manipulations that affect microglial function. One explanation for these findings is that normal microglial activity is required for the induction and/or maintenance of *in vitro* LTF and that either its activation or its inhibition drives microglia away from this normal regulation. This shared effect would be enough to inhibit *in vitro* LTF but, due to the variety of cellular mechanisms affected by the experimental manipulations used, these pharmacological treatments produce not identical effects on burst frequency or amplitude, even for drugs that are similarly categorized (*i.e.* "activators" or "inhibitors"). An alternative explanation is that the pharmacological manipulations used in this study affect a variety of cell mechanisms, not necessarily limited to microglial function, that end up inhibiting the induction and/or maintenance of *in vitro* LTF.

Here we corroborated that application of IH to the preBötC isolated in a brainstem slice preparation produces a long-lasting increase in the respiratory rhythm frequency (Blitz and Ramirez, 2002), which constitutes an *in vitro* LTF. To the best of our knowledge, there are only two reports (including this one) showing that IH induces preBötC plasticity, which contrast with the extensive evidence of IH-induced LTF of a variety of respiratory motor outputs, mainly the phrenic nerve (MacFarlane et al., 2008, 2009; Navarrete-Opazo and Mitchell, 2014; Agosto-Marlin et al., 2017). As already mentioned, pLTF is a very complex phenomenon that includes changes in burst frequency and amplitude, mainly produced by plastic changes at the motor neuron level (MacFarlane et al., 2008, 2009; Navarrete-Opazo and Mitchell, 2014). These changes can be dependent on either adenosinergic or serotonergic modulation (MacFarlane et al., 2008, 2009; Navarrete-Opazo and Mitchell, 2014; Agosto-Marlin et al., 2017). Extensive research is needed to begin comparing *in vitro* LTF with the different forms and mechanisms of pLTF. Moreover, our finding that microglia modulate *in vitro* LTF does not necessarily mean that this is the case for pLTF. The interpretations of our findings obtained *in vitro* must also consider the caveat that microglia might change in slice preparations (Stence et al., 2001; Brawek et al., 2017). The process to obtain the slices and maintain them *in vitro* may induce their activation (Stence et al., 2001; Brawek et al., 2017), mainly on the surface of the slice (Stence et al., 2001; Bernier et al., 2014; Brawek et al., 2017).

Even though the pharmacological profiles of all drugs used in this study share microglia as their common target (Möller et al., 2016; Peña-Ortega, 2017), it must be acknowledged that none of them is completely specific to microglia (Möller et al., 2016; Peña-Ortega, 2017) and that they affect a wide variety of cellular mechanisms (Nikodemova et al., 2006; Möller et al., 2016; Peña-Ortega, 2017), which could produce not identical changes in burst frequency and/or amplitude. It must be noticed that the reduction of respiratory burst amplitude upon the application of all microglial modulators tested here closely reproduces our own previous findings (Lorea-Hernández et al., 2016), which indicate that, despite the type of pharmacological modulation, changing microglial function consistently impacts neural network mechanisms controlling respiratory burst amplitude (Lorea-Hernández et al., 2016) or duration (Lu et al., 2012). However, the effects of these same modulators on respiratory rhythm frequency are highly variable, as previously described (Lu et al., 2012; Lorea-Hernández et al., 2016). It is possible that the non-microglial-mediated effects of these drugs could contribute to the later variability in a preparation-by-preparation basis. The microglial activators used in this study act through different receptors and activate different transductions pathways (Peña-Ortega, 2017). Despite the fact that the major LPS receptor TLR4 is abundantly expressed in microglia (Lehnardt et al., 2003; Song et al., 2011; Lin et al., 2012), it has also been found in some neurons (Tang et al., 2008), mainly under pro-inflammatory conditions (Tang et al., 2008) and in some astrocytes (El-Hage et al., 2011), always in smaller amounts to those in microglia (Song et al., 2011; Lin et al., 2012). Similarly, the fractalkine receptor CX3CR1 is almost exclusively expressed in microglia (Harrison et al., 1998; Meucci et al., 1998). However, its expression has also been reported in subsets of neurons (Hughes et al., 2002; Meucci et al., 1998) and in cultured astrocytes (Maciejewski-Lenoir et al., 1999). The microglial inhibitors used in this study act through different cellular targets (Peña-Ortega, 2017). Fucoidan is an unspecific scavenger receptor antagonist that can certainly inhibit microglia (Do et al., 2010; Peña-Ortega, 2017), but scavenger receptors are also expressed in astrocytes (Alarcón et al., 2005). Minocycline has classically been defined as a "microglial inhibitor" (Möller et al., 2016; Peña-Ortega, 2017), but recent evidence indicates that it could directly or indirectly affect astrocytes, oligodendrocytes and neurons (Möller et al., 2016; Choi et al., 2015). Finally, although the liposomal preparation of clodronate seems to constitute a specific microglial toxin (Kumamaru et al., 2012), clodronate in its free form (non-encapsulated in liposomes) could damage astrocytes (van Neerven et al., 2010; Kumamaru et al., 2012). Thus, although our results indicate that microglia could modulate *in vitro* LTF, we cannot discard that the effects achieved by the pharmacological tools used in this study could also involve changes in other cell types, including other kinds of glia or even neurons (Möller et al., 2016; Peña-Ortega, 2017).

Without ignoring the caveats mentioned in the previous paragraphs, our data suggest that normal microglial activity is required for the induction and/or maintenance of *in vitro* LTF. However, based on the findings that fucoidan and minocycline are anti-inflammatory drugs with inhibitory effects on microglia (Do et al., 2010; Möller et al., 2016) and that LPS and fractalkine are pro-inflammatory drugs with microglial activating properties (Peña-Ortega, 2017), it was expected that both groups of drugs would have opposite effects on *in vitro* LTF. Thus, the finding that all these microglial modulators, as well as the microglial toxin liposomal clodronate, inhibit *in vitro* LTF suggests a more complex scenario. First of all, it has to be considered that microglia can exhibit a variety of phenotypes which are not entirely described by the classic M0, M1 and M2 phenotypes and that these phenotypes can coexist even in the absence of inflammation (Cherry et al., 2014; Shigemoto-Mogami et al., 2014; Peña-Ortega, 2017). The simplest explanation for the apparent contradiction raised by the similar effects of microglial inhibitors and activators is that all pharmacological manipulations tested in this study have a shared effect on microglia under our experimental conditions. For instance, fractalkine, which was considered here as a microglial activator (Sun et al., 2015), can produce anti-inflammatory effects (Lyons et al., 2009; Ślusarczyk et al., 2016) and even inhibit microglial activity (Lyons et al., 2009; Ślusarczyk et al., 2016). In contrast, the variety of pharmacological manipulations used in this study to inhibit or deplete microglia could also have pro-inflammatory effects (Jin and Yu, 2015; Vetvicka and Vetvickova, 2017). For instance, fucoidan normally inhibits the activation of immune-responsive cells, including microglia (Do et al., 2010), but it can have activating effects on macrophages and neutrophils, contributing to the release of pro-inflammatory mediators, including cytokines (Do et al., 2010; Jin and Yu, 2015; Stefaniak–Vidarsson et al., 2017; Vetvicka and Vetvickova, 2017), in a similar fashion to LPS (Jin and Yu, 2015; Vetvicka and Vetvickova, 2017). Regarding other similarities with LPS, fucoidan can induce toxic effects on microglia at a slightly higher dose than the one used in our study (50 μg/ml; Do et al., 2010), which coincides with the toxicity that high concentrations of LPS can have on microglia (Mayo and Stein, 2007; Wu et al., 2015; Chan et al., 2017). Similarly, aside from its anti-inflammatory and antioxidant effects (Möller et al., 2016; Peña-Ortega, 2017), minocycline can induce

paradoxical microglial activation in the developing brain (Arnoux et al., 2014; Strahan et al., 2017) that could increase pro-inflammatory cytokine release (Zhao et al., 2015). The paradoxical minocycline-induced microglial activation in the developing brain is relevant for this study considering that we used slices obtained from neonates for the experiments. Another similarity is that minocycline can be pro-apoptotic (Ueno et al., 2013; Arnoux et al., 2014; Inta et al., 2016; Strahan et al., 2017) like LPS (Mayo and Stein, 2007). Treatment with liposomal clodronate can also have similar effects to those induced by LPS since liposomes, regardless of their content, can induce early inflammation (Pervin et al., 2016). Furthermore, derivatives of phosphatidylcholine (i.e., lysophosphatidylcholine), the main lipid used in our liposomal preparation, can induce microglial activation (Schilling et al., 2004; Scholz and Eder, 2017). Microglial activation can be also induced by cholesterol (Xue et al., 2007), the other lipid used in our liposomal preparation. Thus, it is possible that all pharmacological manipulations used in this study could lead to some degree of microglial activation and/or toxicity, which produces a similar inhibition of *in vitro* LTF. It must be acknowledged that minocycline (Zhou et al., 2011) and cholesterol (Koudinov and Koudinova, 2003) inhibit other plastic changes in neural circuits, such as LTP, which is also inhibited by LPS (Nolan et al., 2004) and fractalkine (Maggi et al., 2009). Regarding breathing, minocycline blocks the respiratory adaptation to sustained hypoxia (Stokes et al., 2017). Therefore, it should not be surprising that both LPS and minocycline inhibit *in vitro* LTF (this study), as has been already reported for pLTF recorded *in vivo*, which is inhibited by systemic application of both LPS and minocycline (Huxtable et al., 2011). However, in this particular case it was suggested that the inhibitory effect of minocycline on pLTF might be due to the inhibition of protein kinase C isoforms (Nikodemova et al., 2006; Huxtable et al., 2011).

Our data could also suggest that the alteration of normal microglial activity either by its activation or by its inhibition could divert them from their normal modulatory function in the preBötC (Lu et al., 2012; Lorea-Hernández et al., 2016). It is possible that the pharmacological manipulations used in this study could lead microglia to different, and perhaps opposite, states that would impede the induction and/or maintenance of *in vitro* LTF by diverse mechanisms, including differential changes in the levels of microglial mediators (Peña-Ortega, 2012). For instance, it is well known that microglial activation leads to IL-1β release (Choi et al., 2015), which could reduce the probability of LTF induction due to its inhibitory effects on breathing (Olsson et al., 2003). This may also be the case for other cytokines or prostaglandins, which are released upon microglial modulation (Allen et al., 1982; Henry et al., 2009; Liu et al., 2012; Elmore et al., 2014) and are known to inhibit breathing (Ballanyi et al., 1997, 1999; Olsson et al., 2003). Alternatively, the inhibition of microglial function could lead to a decrease in the release of molecules that promote breathing generation and whose reduced modulation could contribute to the inhibition of LTF induction (MacFarlane et al., 2008, 2009; Peña-Ortega, 2012; Pardo-Peña et al., 2016). For instance, it is well known that ROS, NO and BDNF are necessary for pLTF induction (MacFarlane et al., 2008, 2009; 2014). ROS, NO and BDNF are constantly released by microglia even in the absence of activating signals (Zhang et al., 2007; Gomes et al., 2013; Quintas et al., 2014; Pardo-Peña et al., 2018). Moreover, they can modulate breathing generation (Pyatin and Miroshnichenko, 2001; Bouvier et al., 2008; Garcia et al., 2011), which opens the possibility that a reduction of the levels of these mediators, as a consequence of microglial inhibition, could contribute to the disturbance of LTF generation *in vitro*. This may also be the case for histamine or prostaglandins that are released by microglia even in resting conditions (Katoh et al., 2001; Zhang et al., 2009; Wang et al., 2011) and that are known to modulate breathing generation (Dutschmann et al., 2003; Koch et al., 2015). To support this possibility, we have recently shown that minocycline reduces the basal extracellular levels of hydrogen peroxide in brainstem slices (Pardo-Peña et al., 2018), which seems to be the case for other pro-inflammatory mediators (Dunston et al., 2011; Kobayashi et al., 2013; Scholz et al., 2015) and neurotrophic factors (Ueno et al., 2013). Even though our findings require a more cell-specific corroboration of the precise role of microglia on LTF *in vitro*, the pharmacological experiments presented in this study strongly suggest that microglia modulate not only basal preBötC activity (Lu et al., 2012; Lorea-Hernández et al., 2016) but also the plastic changes that this circuit undergoes in response to IH. Microglial modulation of respiratory rhythm plasticity has to be considered when treating conditions associated with IH, such as sleep apneas (MacFarlane et al., 2008, 2009; Navarrete-Opazo and Mitchell, 2014), or in therapeutic approaches that use IH as a beneficial tool (Dale et al., 2014; Gonzalez-Rothi et al., 2015).

Conflicts of interest

The authors have no conflict of interest to declare.

Acknowledgements

The authors thank Jessica González Norris for editorial comments. We thank Benito Ordaz for technical support. Camacho-Hernández Neira Polet and Lorea-Hernández Jonathan Julio are PhD students at UNAM and receive fellowships from CONACyT. This study was supported by Fundación Marcos Moshinsky, CONACyT Grants 117 and 235789; and by DGAPA-UNAM Grant IN202018.

References

Agosto-Marlin, I.M., Nichols, N.L., Mitchell, G.S., 2017. Adenosine-dependent phrenic motor facilitation is inflammation resistant. J. Neurophysiol. 117, 836–845.
Alarcón, R., Fuenzalida, C., Santibáñez, M., von Bernhardi, R., 2005. Expression of scavenger receptors in glial cells. Comparing the adhesion of astrocytes and microglia from neonatal rats to surface-bound beta-amyloid. J. Biol. Chem. 280, 30406–30415.
Allen, L.G., Louis, T.M., Kopelman, A.E., 1982. Brain prostaglandins E2 and F2 alpha following neonatal asphyxia in the guinea pig. Biol. Neonate 42, 8–14.
Arnoux, I., Hoshiko, M., Sanz Diez, A., Audinat, E., 2014. Paradoxical effects of minocycline in the developing mouse somatosensory cortex. Glia 62, 399–410.
Balan, K.V., Kc, P., Hoxha, Z., Mayer, C.A., Wilson, C.G., Martin, R.J., 2011. Vagal afferents modulate cytokine-mediated respiratory control at the neonatal medulla oblongata. Respir. Physiol. Neurobiol. 178, 458–464.
Ballanyi, K., Lalley, P.M., Hoch, B., Richter, D.W., 1997. cAMP-dependent reversal of opioid- and prostaglandin-mediated depression of the isolated respiratory network in newborn rats. J. Physiol. 504, 127–134.
Ballanyi, K., Onimaru, H., Homma, I., 1999. Respiratory network function in the isolated brainstem-spinal cord of newborn rats. Prog. Neurobiol. 59, 583–634.
Banks, W.A., Ortiz, L., Plotkin, S.R., Kastin, A.J., 1991. Human interleukin (IL) 1 alpha, murine IL-1 alpha and murine IL-1 beta are transported from blood to brain in the mouse by a shared saturable mechanism. J. Pharmacol. Exp. Ther. 259, 988–996.
Banks, W.A., Kastin, A.J., Ehrensing, C.A., 1994. Blood-borne interleukin-1 alpha is transported across the endothelial blood-spinal cord barrier of mice. J Physiol. 479, 257–264.
Blitz, D.M., Ramirez, J.M., 2002. Long-term modulation of respiratory network activity following anoxia in vitro. J. Neurophysiol. 87, 2964–2971.
Bluthé, R.M., Michaud, B., Kelley, K.W., Dantzer, R., 1996. Vagotomy attenuates behavioural effects of interleukin-1 injected peripherally but not centrally. Neuroreport 7, 1485–1488.
Bouvier, J., Autran, S., Dehorter, N., Katz, D., Champagnat, J., Fortin, G., Thoby-Brisson, M., 2008. Brain-derived neurotrophic factor enhances fetal respiratory rhythm frequency in the mouse preBötzinger complex in vitro. Eur. J. Neurosci. 28, 510–520.
Brawek, B., Liang, Y., Savitska, D., Li, K., Fomin-Thunemann, N., Kovalchuk, Y., Zirdum, E., Jakobsson, J., Garaschuk, O., 2017. A new approach for ratiometric in vivo calcium imaging of microglia. Sci. Rep. 7, 6030.
Chan, C.K., Tan, L.T., Andy, S.N., Kamarudin, M.N.A., Goh, B.H., Kadir, H.A., 2017. Anti-neuroinflammatory activity of Elephantopus scaber L. Via activation of Nrf2/HO-1 signaling and inhibition of p38 MAPK pathway in LPS-Induced microglia BV-2 cells. Front. Pharmacol. 8, 397.
Choi, H.S., Roh, D.H., Yoon, S.Y., Moon, J.Y., Choi, S.R., Kwon, S.G., Kang, S.Y., Han, H.J., Kim, H.W., Beitz, A.J., Oh, S.B., Lee, J.H., 2015. Microglial interleukin-1β in the ipsilateral dorsal horn inhibits the development of mirror-image contralateral mechanical allodynia through astrocyte activation in a rat model of inflammatory pain. Pain 156, 1046–1059.
Dale, E.A., Ben Mabrouk, F., Mitchell, G.S., 2014. Unexpected benefits of intermittent hypoxia: enhanced respiratory and nonrespiratory motor function. Physiology (Bethesda) 29, 39–48.
Do, H., Kang, N.S., Pyo, S., Billiar, T.R., Sohn, E.H., 2010. Differential regulation by fucoidan of IFN-γ-induced NO production in glial cells and macrophages. J. Cell. Biochem. 111, 1337–1345.

Dunston, C.R., Griffiths, H.R., Lambert, P.A., Staddon, S., Vernallis, A.B., 2011. Proteomic analysis of the anti-inflammatory action of minocycline. Proteomics 11, 42–51.
Dutschmann, M., Bischoff, A.M., Büsselberg, D., Richter, D.W., 2003. Histaminergic modulation of the intact respiratory network of adult mice. Pflug. Arch. 445, 570–576.
Ek, M., Kurosawa, M., Lundeberg, T., Ericsson, A., 1998. Activation of vagal afferents after intravenous injection of interleukin-1beta: role of endogenous prostaglandins. J. Neurosci. 18, 9471–9479.
El-Hage, N., Podhaizer, E.M., Sturgill, J., Hauser, K.F., 2011. Toll-like receptor expression and activation in astroglia: differential regulation by HIV-1 Tat, gp120, and morphine. Immunol. Invest. 40, 498–522.
Elmore, M.R., Burton, M.D., Conrad, M.S., Rytych, J.L., Van Alstine, W.G., Johnson, R.W., 2014. Respiratory viral infection in neonatal piglets causes marked microglia activation in the hippocampus and deficits in spatial learning. J. Neurosci. 34, 2120–2129.
Engblom, D., Ek, M., Andersson, I.M., Saha, S., Dahlström, M., Jakobsson, P.J., Ericsson-Dahlstrand, A., Blomqvist, A., 2002. Induction of microsomal prostaglandin E synthase in the rat brain endothelium and parenchyma in adjuvant-induced arthritis. J. Comp. Neurol. 452, 205–214.
Garcia 3rd, A.J., Khan, S.A., Kumar, G.K., Prabhakar, N.R., Ramirez, J.M., 2011. Hydrogen peroxide differentially affects activity in the pre-Bötzinger complex and hippocampus. J. Neurophysiol. 106, 3045–3055.
Goehler, L.E., Gaykema, R.P., Opitz, N., Reddaway, R., Badr, N., Lyte, M., 2005. Activation in vagal afferents and central autonomic pathways: early responses to intestinal infection with Campylobacter jejuni. Brain Behav. Immun. 19, 334–344.
Gomes, C., Ferreira, R., George, J., Sanches, R., Rodrigues, D.I., Gonçalves, N., Cunha, R.A., 2013. Activation of microglial cells triggers a release of brain-derived neurotrophic factor (BDNF) inducing their proliferation in an adenosine A2A receptor-dependent manner: A2A receptor blockade prevents BDNF release and proliferation of microglia. J. Neuroinflamm. 10, 16.
Gonzalez-Rothi, E.J., Lee, K.Z., Dale, E.A., Reier, P.J., Mitchell, G.S., Fuller, D., 1985. Intermittent hypoxia and neurorehabilitation. J. Appl. Physiol. 119, 1455–1465.
Harrison, J.K., Jiang, Y., Chen, S., Xia, Y., Maciejewski, D., McNamara, R.K., Streit, W.J., Salafranca, M.N., Adhikari, S., Thompson, D.A., Botti, P., Bacon, K.B., Feng, L., 1998. Role for neuronally derived fractalkine in mediating interactions between neurons and CX3CR1-expressing microglia. Proc. Natl. Acad. Sci. U. S. A. 95, 10896–10901.
Henry, C., Huang, Y., Wynne, A., Godbout, J., 2009. Peripheral lipopolysaccharide (LPS) challenge promotes microglial hyperactivity in aged mice that is associated with exaggerated induction of both pro-inflammatory IL-1beta and anti-inflammatory IL-10 cytokines. Brain Behav. Immun. 23, 309–317.
Herlenius, E., 2011. An inflammatory pathway to apnea and autonomic dysregulation. Respir. Physiol. Neurobiol. 178, 449–457.
Hughes, P.M., Botham, M.S., Frentzel, S., Mir, A., Perry, V.H., 2002. Expression of fractalkine (CX3CL1) and its receptor, CX3CR1, during acute and chronic inflammation in the rodent CNS. Glia 37, 314–327.
Huxtable, A.G., Vinit, S., Windelborn, J.A., Crader, S.M., Guenther, C.H., Watters, J.J., Mitchell, G.S., 2011. Systemic inflammation impairs respiratory chemoreflexes and plasticity. Respir. Physiol. Neurobiol. 178, 482–489.
Huxtable, A.G., Smith, S.M., Vinit, S., Watters, J.J., Mitchell, G.S., 2013. Systemic LPS induces spinal inflammatory gene expression and impairs phrenic long-term facilitation following acute intermittent hypoxia. J. Appl. Physiol. (1985) 114, 879–887.
Huxtable, A.G., Smith, S.M., Peterson, T.J., Watters, J.J., Mitchell, G.S., 2015. Intermittent hypoxia-induced spinal inflammation impairs respiratory motor plasticity by a spinal p38 MAP kinase-dependent mechanism. J. Neurosci. 35, 6871–6880.
Huxtable, A.G., Kopp, E., Doughtery, B.J., Watters, J.J., Mitchell, G.S., 2018. Cyclooxygenase enzyme activity does not impair respiratory motor plasticity after one night of intermittent hypoxia. Respir. Physiol. Neurobiol (in press).
Inta, I., Vogt, M.A., Vogel, A.S., Bettendorf, M., Gass, P., Inta, D., 2016. Minocycline exacerbates apoptotic neurodegeneration induced by the NMDA receptor antagonist MK-801 in the early postnatal mouse brain. Eur. Arch. Psychiatry Clin. Neurosci. 266, 673–677.
Jin, J.O., Yu, Q., 2015. Fucoidan delays apoptosis and induces pro-inflammatory cytokine production in human neutrophils. Int. J. Biol. Macromol. 73, 65–71.
Johnson, S.M., Randhawa, K.S., Epstein, J.J., Gustafson, E., Hocker, A.D., Huxtable, A.G., Baker, T.L., Watters, J.J., 2018. Gestational intermittent hypoxia increases susceptibility to neuroinflammation and alters respiratory motor control in neonatal rats. Respir. Physiol. Neurobiol (in press).
Katoh, Y., Niimi, M., Yamamoto, Y., Kawamura, T., Morimoto-Ishizuka, T., Sawada, M., Takemori, H., Yamatodani, A., 2001. Histamine production by cultured microglial cells of the mouse. Neurosci. Lett. 305, 181–184.
Kobayashi, K., Imagama, S., Ohgomori, T., Hirano, K., Uchimura, K., Sakamoto, K., Hirakawa, A., Takeuchi, H., Suzumura, A., Ishiguro, N., Kadomatsu, K., 2013. Minocycline selectively inhibits M1 polarization of microglia. Cell Death Dis. 4, e525.
Koch, H., Caughie, C., Elsen, F.P., Doi, A., Garcia 3rd, A.J., Zanella, S., Ramirez, J.M., 2015. Prostaglandin E2 differentially modulates the central control of eupnoea, sighs and gasping in mice. J. Physiol. 593, 305–319.
Koudinov, A.R., Koudinova, N.V., 2003. Cholesterol, synaptic function and Alzheimer's disease. Pharmacopsychiatry 36, S107–12.
Kumamaru, H., Saiwai, H., Kobayakawa, K., Kubota, K., van Rooijen, N., Inoue, K., Iwamoto, Y., Okada, S., 2012. Liposomal clodronate selectively eliminates microglia from primary astrocyte cultures. J. Neuroinflamm. 9, 116.
Layé, S., Bluthé, R.M., Kent, S., Combe, C., Médina, C., Parnet, P., Kelley, K., Dantzer, R., 1995. Subdiaphragmatic vagotomy blocks induction of IL-1 beta mRNA in mice brain in response to peripheral LPS. Am. J. Physiol. 268, R1327–31.
Lehnardt, S., Massillon, L., Follett, P., Jensen, F.E., Ratan, R., Rosenberg, P.A., Volpe, J.J., Vartanian, T., 2003. Activation of innate immunity in the CNS triggers neurodegeneration through a Toll-like receptor 4-dependent pathway. Proc. Natl. Acad. Sci. U. S. A. 100, 8514–8519.
Lin, S., Yin, Q., Zhong, Q., Lv, F.L., Zhou, Y., Li, J.Q., Wang, J.Z., Su, B.Y., Yang, Q.W., 2012. Heme activates TLR4-mediated inflammatory injury via MyD88/TRIF signaling pathway in intracerebral hemorrhage. J. Neuroinflamm. 9, 46.
Liu, X., Wu, Z., Hayashi, Y., Nakanishi, H., 2012. Age-dependent neuroinflammatory responses and deficits in long-term potentiation in the hippocampus during systemic inflammation. Neuroscience 216, 133–142.
Lorea-Hernández, J.J., Morales, T., Rivera-Angulo, A.J., Alcantara-Gonzalez, D., Peña-Ortega, F., 2016. Microglia modulate respiratory rhythm generation and autoresuscitation. Glia 64, 603–619.
Lu, A.D., Wang, J.F., Chen, Y.H., Hou, L.L., Zhou, X.J., Bian, J.J., Wang, J.J., Zhu, K.M., 2012. Nitric oxide and ATP-sensitive potassium channels mediate lipopolysaccharide-induced depression of central respiratory-like activity in brain slices. Neurosignals 20, 103–111.
Lyons, A., Lynch, A.M., Downer, E.J., Hanley, R., O'Sullivan, J.B., Smith, A., Lynch, M.A., 2009. Fractalkine-induced activation of the phosphatidylinositol-3 kinase pathway attentuates microglial activation in vivo and in vitro. J. Neurochem. 110, 1547–1556.
MacFarlane, P.M., Wilkerson, J.E., Lovett-Barr, M.R., Mitchell, G.S., 2008. Reactive oxygen species and respiratory plasticity following intermittent hypoxia. Respir. Physiol. Neurobiol. 164, 263–271.
MacFarlane, P.M., Satriotomo, I., Windelborn, J.A., Mitchell, G.S., 2009. NADPH oxidase activity is necessary for acute intermittent hypoxia-induced phrenic long-term facilitation. J. Physiol. 587, 1931–1942.
MacFarlane, P.M., Vinit, S., Mitchell, G.S., 2014. Spinal nNOS regulates phrenic motor facilitation by a 5-HT2B receptor- and NADPH oxidase-dependent mechanism. Neuroscience 269, 67–78.
Maciejewski-Lenoir, D., Chen, S., Feng, L., Maki, R., Bacon, K.B., 1999. Characterization of fractalkine in rat brain cells: migratory and activation signals for CX3CR-1-expressing microglia. J. Immunol. 163, 1628–1635.
Maggi, L., Trettel, F., Scianni, M., Bertollini, C., Eusebi, F., Fredholm, B.B., Limatola, C., 2009. LTP impairment by fractalkine/CX3CL1 in mouse hippocampus is mediated through the activity of adenosine receptor type 3 (A3R). J. Neuroimmunol. 215, 36–42.
Matsukawa, N., Yasuhara, T., Hara, K., Xu, L., Maki, M., Yu, G., Kaneko, Y., Ojika, K., Hess, D.C., Borlongan, C.V., 2009. Therapeutic targets and limits of minocycline neuroprotection in experimental ischemic stroke. BMC Neurosci. 10, 126.
Mayer, A.M., Hall, M.L., Holland, M., De Castro, C., Molinaro, A., Aldulescu, M., Frenkel, J., Ottenhoff, L., Rowley, D., Powell, J., 2014. Vibrio vulnificus MO6-24/O lipopolysaccharide stimulates superoxide anion, thromboxane B_2, matrix metalloproteinase-9, cytokine and chemokine release by rat brain microglia in vitro. Mar. Drugs 12, 1732–1756.
Mayo, L., Stein, R., 2007. Characterization of LPS and interferon-gamma triggered activation-induced cell death in N9 and primary microglial cells: induction of the mitochondrial gateway by nitric oxide. Cell Death Differ. 14, 183–186.
Meucci, O., Fatatis, A., Simen, A.A., Bushell, T.J., Gray, P.W., Miller, R.J., 1998. Chemokines regulate hippocampal neuronal signaling and gp120 neurotoxicity. Proc. Natl. Acad. Sci. U. S. A. 95, 14500–14505.
Möller, T., Bard, F., Bhattacharya, A., Biber, K., Campbell, B., Dale, E., Eder, C., Gan, L., Garden, G.A., Hughes, Z.A., Pearse, D.D., Staal, R.G., Sayed, F.A., Wes, P.D., Boddeke, H.W., 2016. Critical data-based re-evaluation of minocycline as a putative specific microglia inhibitor. Glia 64, 1788–1794.
Navarrete-Opazo, A., Mitchell, G.S., 2014. Therapeutic potential of intermittent hypoxia: a matter of dose. Am. J. Physiol. Regul. Integr. Comp. Physiol. 307, R1181–1197.
Nikodemova, M., Duncan, I.D., Watters, J.J., 2006. Minocycline exerts inhibitory effects on multiple mitogen-activated protein kinases and IkappaBalpha degradation in a stimulus-specific manner in microglia. J. Neurochem. 96, 314–323.
Nolan, Y., Martin, D., Campbell, V.A., Lynch, M.A., 2004. Evidence of a protective effect of phosphatidylserine-containing liposomes on lipopolysaccharide-induced impairment of long-term potentiation in the rat hippocampus. J. Neuroimmunol. 151, 12–23.
Olsson, A., Kayhan, G., Lagercrantz, H., Herlenius, E., 2003. IL-1 beta depresses respiration and anoxic survival via a prostaglandin-dependent pathway in neonatal rats. Pediatr. Res. 54, 326–331.
Pardo-Peña, K., Peña-Ortega, F., Morales-Villagrán, A., Camacho-Hernández, P., Lorea-Hernández, J.J., 2016. Measurements of hydrogen peroxide in line and their change by hypoxia and microglia modulation. Neuroscience Meeting Planner Online.
Pardo-Peña, K., Lorea-Hernández, J.J., Camacho-Hernández, N.P., Ordaz, B., Villasana-Salazar, B., Morales-Villagrán, A., Peña-Ortega, F., 2018. Hydrogen peroxide extracellular concentration in the ventrolateral medulla and its increase in response to hypoxia in vitro: possible role of microglia. Brain Res. 1692, 87–99.
Peña-Ortega, F., 2012. Tonic neuromodulation of the inspiratory rhythm generator. Front. Physiol. 3, 253.
Peña, F., Parkis, M.A., Tryba, A.K., Ramirez, J.M., 2004. Differential contribution of pacemaker properties to the generation of respiratory rhythms during normoxia and hypoxia. Neuron 43, 105–117.
Peña, F., Meza-Andrade, R., Páez-Zayas, V., González-Marín, M.C., 2008. Gasping generation in developing Swiss-Webster mice in vitro and in vivo. Neurochem. Res. 33, 1492–1500.
Peña-Ortega, F., 2017. Pharmacological tools to activate microglia and their possible use to study neural network patho-physiology. Curr. Neuropharmacol. 15, 595–619.
Pervin, M., Golbar, H.M., Bondoc, A., Izawa, T., Kuwamura, M., Yamate, J., 2016. Transient effects of empty liposomes on hepatic macrophage populations in rats. J. Toxicol. Pathol. 29, 139–144.
Pyatin, V.F., Miroshnichenko, I.V., 2001. Effects of nitric oxide on respiratory activity in bulbospinal preparation from rat fetus. Bull. Exp. Biol. Med. 132, 723–726.

Quintas, C., Pinho, D., Pereira, C., Saraiva, L., Gonçalves, J., Queiroz, G., 2014. Microglia $P2Y_6$ receptors mediate nitric oxide release and astrocyte apoptosis. J. Neuroinflamm. 11, 141.
Ramírez-Jarquín, J.O., Lara-Hernández, S., López-Guerrero, J.J., Aguileta, M.A., Rivera-Angulo, A.J., Sampieri, A., Vaca, L., Ordaz, B., Peña-Ortega, F., 2012. Somatostatin modulates generation of inspiratory rhythms and determines asphyxia survival. Peptides 34, 360.
Schilling, T., Lehmann, F., Rückert, B., Eder, C., 2004. Physiological mechanisms of lysophosphatidylcholine-induced de-ramification of murine microglia. J. Physiol. 557, 105–120.
Scholz, H., Eder, C., 2017. Lysophosphatidylcholine activates caspase-1 in microglia via a novel pathway involving two inflammasomes. J. Neuroimmunol. 310, 107–110.
Scholz, R., Sobotka, M., Caramoy, A., Stempfl, T., Moehle, C., Langmann, T., 2015. Minocycline counter-regulates pro-inflammatory microglia responses in the retina and protects from degeneration. J. Neuroinflamm. 12, 209.
Shigemoto-Mogami, Y., Hoshikawa, K., Goldman, J.E., Sekino, Y., Sato, K., 2014. Microglia enhance neurogenesis and oligodendrogenesis in the early postnatal subventricular zone. J. Neurosci. 34, 2231–2243.
Ślusarczyk, J., Trojan, E., Głombik, K., Chamera, K., Roman, A., Budziszewska, B., Basta-Kaim, A., 2016. Fractalkine attenuates microglial cell activation induced by prenatal stress. Neural Plast. 2016, 7258201.
Song, M., Jin, J., Lim, J.E., Kou, J., Pattanayak, A., Rehman, J.A., Kim, H.D., Tahara, K., Lalonde, R., Fukuchi, K., 2011. TLR4 mutation reduces microglial activation, increases Aβ deposits and exacerbates cognitive deficits in a mouse model of Alzheimer's disease. J. Neuroinflamm. 8, 92.
Stefaniak–Vidarsson, M.M., Gudjónsdóttir, M., Marteinsdottir, G., Sigurjonsson, O.E., Kristbergsson, K., 2017. Evaluation of bioactivity of fucoidan from laminaria with in vitro human cell culture (THP-1). Funct. Foods Health Dis. 7, 688–701.
Stence, N., Waite, M., Dailey, M.E., 2001. Dynamics of microglial activation: a confocal time-lapse analysis in hippocampal slices. Glia 33, 256–266.
Stokes, J.A., Arbogast, T.E., Moya, E.A., Fu, Z., Powell, F.L., 2017. Minocycline blocks glial cell activation and ventilatory acclimatization to hypoxia. J. Neurophysiol. 117, 1625–1635.
Strahan, J.A., Walker 2nd, W.H., Montgomery, T.R., Forger, N.G., 2017. Minocycline causes widespread cell death and increases microglial labeling in the neonatal mouse brain. Dev. Neurobiol. 77, 753–766.
Sun, S., Yu, H., Yu, H., Honglin, M., Ni, W., Zhang, Y., Guo, L., He, Y., Xue, Z., Ni, Y., Li, J., Feng, Y., Chen, Y., Shao, R., Chai, R., Li, H., 2015. Inhibition of the activation and recruitment of microglia-like cells protects against neomycin-induced ototoxicity. Mol. Neurobiol. 51, 252–267.
Tadmouri, A., Champagnat, J., Morin-Surun, M.P., 2014. Activation of microglia and astrocytes in the nucleus tractus solitarius during ventilatory acclimatization to 10% hypoxia in unanesthetized mice. J. Neurosci. Res. 92, 627–633.
Tang, S.C., Lathia, J.D., Selvaraj, P.K., Jo, D.G., Mughal, M.R., Cheng, A., Siler, D.A., Markesbery, W.R., Arumugam, T.V., Mattson, M.P., 2008. Toll-like receptor-4 mediates neuronal apoptosis induced by amyloid beta-peptide and the membrane lipid peroxidation product 4-hydroxynonenal. Exp. Neurol. 213, 114–121.
Tryba, A.K., Peña, F., Ramirez, J.M., 2003. Stabilization of bursting in respiratory pacemaker neurons. J. Neurosci. 23, 3538–3546.
Ueno, M., Fujita, Y., Tanaka, T., Nakamura, Y., Kikuta, J., Ishii, M., Yamashita, T., 2013. Layer V cortical neurons require microglial support for survival during postnatal development. Nat. Neurosci. 16, 543–551.
van Neerven, S., Nemes, A., Imholz, P., Regen, T., Denecke, B., Johann, S., Beyer, C., Hanisch, U.K., Mey, J., 2010. Inflammatory cytokine release of astrocytes in vitro is reduced by all-trans retinoic acid. J. Neuroimmunol. 229, 169–179.
van Rooijen, N., Sanders, A., 1996. Kupffer cell depletion by liposome-delivered drugs: comparative activity of intracellular clodronate, propamidine, and ethylenediaminetetraacetic acid. Hepatology 23, 1239–1243.
Vetvicka, V., Vetvickova, J., 2017. Fucoidans stimulate immune reaction and suppress Cancer growth. Anticancer Res. 37, 6041–6046.
Vinit, S., Windelborn, J.A., Mitchell, G.S., 2011. Lipopolysaccharide attenuates phrenic long-term facilitation following acute intermittent hypoxia. Respir. Physiol. Neurobiol. 176, 130–135.
Wang, F., Wu, H., Xu, S., Guo, X., Yang, J., Shen, X., 2011. Macrophage migration inhibitory factor activates cyclooxygenase 2-prostaglandin E2 in cultured spinal microglia. Neurosci. Res. 71, 210–218.
Wu, W.Y., Wu, Y.Y., Huang, H., He, C., Li, W.Z., Wang, H.L., Chen, H.Q., Yin, Y.Y., 2015. Biochanin A attenuates LPS-induced pro-inflammatory responses and inhibits the activation of the MAPK pathway in BV2 microglial cells. Int. J. Mol. Med. 35, 391–398.
Wuchert, F., Ott, D., Murgott, J., Rafalzik, S., Hitzel, N., Roth, J., Gerstberger, R., 2008. Rat area postrema microglial cells act as sensors for the toll-like receptor-4 agonist lipopolysaccharide. J. Neuroimmunol. 204, 66–74.
Wuchert, F., Ott, D., Rafalzik, S., Roth, J., Gerstberger, R., 2009. Tumor necrosis factor-alpha, interleukin-1beta and nitric oxide induce calcium transients in distinct populations of cells cultured from the rat area postrema. J. Neuroimmunol. 206, 44–51.
Xue, Q.S., Sparks, D.L., Streit, W.J., 2007. Microglial activation in the hippocampus of hypercholesterolemic rabbits occurs independent of increased amyloid production. J. Neuroinflamm. 4, 20.
Zavala-Tecuapetla, C., Aguileta, M.A., Lopez-Guerrero, J.J., González-Marín, M.C., Peña, F., 2008. Calcium-activated potassium currents differentially modulate respiratory rhythm generation. Eur. J. Neurosci. 27, 2871–2884.
Zavala-Tecuapetla, C., Tapia, D., Rivera-Angulo, A.J., Galarraga, E., Peña-Ortega, F., 2014. Morphological characterization of respiratory neurons in the pre-Bötzinger complex. Prog. Brain Res. 209, 39–56.
Zhang, P., Hatter, A., Liu, B., 2007. Manganese chloride stimulates rat microglia to release hydrogen peroxide. Toxicol. Lett. 173, 88–100.
Zhang, D., Hu, X., Qian, L., Wilson, B., Lee, C., Flood, P., Langenbach, R., Hong, J.S., 2009. Prostaglandin E2 released from activated microglia enhances astrocyte proliferation in vitro. Toxicol. Appl. Pharmacol. 238, 64–70.
Zhao, Q., Xie, X., Fan, Y., Zhang, J., Jiang, W., Wu, X., Yan, S., Chen, Y., Peng, C., You, Z., 2015. Phenotypic dysregulation of microglial activation in young offspring rats with maternal sleep deprivation-induced cognitive impairment. Sci. Rep. 5, 9513.
Zhou, L.J., Yang, T., Wei, X., Liu, Y., Xin, W.J., Chen, Y., Pang, R.P., Zang, Y., Li, Y.Y., Liu, X.G., 2011. Brain-derived neurotrophic factor contributes to spinal long-term potentiation and mechanical hypersensitivity by activation of spinal microglia in rat. Brain Behav. Immun. 25, 322–334.